



Acyltransferase Anil, a Tailoring Enzyme with Broad Substrate Tolerance for High-Level Production of Anisomycin

Qing Wang,^a Lingxin Kong,^a Xiaoqing Zheng,^a Jufang Shen,^a Junbo Wang,^a Dashan Zhang,^a Yongjian Qiao,^a Jinjin Wang,^a Zixin Deng,^a  Delin You^a

^aState Key Laboratory of Microbial Metabolism, Joint International Research Laboratory of Metabolic and Developmental Sciences, School of Life Sciences & Biotechnology, Shanghai Jiao Tong University, Shanghai, China

Qing Wang and Lingxin Kong contributed equally to this work. The order was determined by the level of contribution to the study.

ABSTRACT Anisomycin (compound 1), a pyrrolidine antibiotic, exhibits diverse biological and pharmacologic activities. The biosynthetic gene cluster of compound 1 has been identified previously, and the multistep assembly of the core benzylpyrrolidine scaffold was characterized. However, enzymatic modifications, such as acylation, involved in compound 1 biosynthesis are unknown. In this study, the genetic manipulation of *anil* proved that it encoded an indispensable acetyltransferase for compound 1 biosynthesis. Bioinformatics analysis suggested Anil as a member of maltose (MAT) and galactoside O-acetyltransferases (GAT) with C-terminal left-handed parallel beta-helix (LbH) subdomain, which were referred to as LbH-MAT-GAT sugar O-acetyltransferases. However, the biochemical assay identified that its target site was the hydroxyl group of the pyrrolidine ring. Anil was found to be tolerant of acyl donors with different chain lengths for the biosynthesis of compound 1 and derivatives 12 and 13 with butyryl and isovaleryl groups, respectively. Meanwhile, it showed comparable activity toward biosynthetic intermediates and synthesized analogues, suggesting promiscuity to the pyrrolidine ring structure of compound 1. These data may inspire new viable synthetic routes for the construction of more complex pyrrolidine ring scaffolds in compound 1. Finally, the overexpression of *anil* under the control of strong promoters contributed to the higher productivities of compound 1 and its analogues. These findings reported here not only improve the understanding of anisomycin biosynthesis but also expand the substrate scope of O-acetyltransferase working on the pyrrolidine ring and pave the way for future metabolic engineering construction of high-yield strains.

IMPORTANCE Acylation is an important tailoring reaction during natural product biosynthesis. Acylation could increase the structural diversity and affect the chemical stability, volatility, biological activity, and even the cellular localization of specialized compounds. Many acetyltransferases have been reported in natural product biosynthesis. The typical example of the LbH-MAT-GAT sugar O-acetyltransferase subfamily was reported to catalyze the coenzyme A (CoA)-dependent acetylation of the 6-hydroxyl group of sugars. However, no protein of this family has been characterized to acetylate a nonsugar secondary metabolic product. Here, Anil was found to catalyze the acylation of the hydroxyl group of the pyrrolidine ring and be tolerant of diverse acyl donors and acceptors, which made the biosynthesis more efficient and exclusive for biosynthesis of compound 1 and its derivatives. Moreover, the overexpression of *anil* serves as a successful example of genetic manipulation of a modification gene for the high production of final products and might set the stage for future metabolic engineering.

KEYWORDS pyrrolidine antibiotic, anisomycin, O-acetyltransferase, acylation, substrate specificity

Citation Wang Q, Kong L, Zheng X, Shen J, Wang J, Zhang D, Qiao Y, Wang J, Deng Z, You D. 2021. Acyltransferase Anil, a tailoring enzyme with broad substrate tolerance for high-level production of anisomycin. *Appl Environ Microbiol* 87:e00172-21. <https://doi.org/10.1128/AEM.00172-21>.

Editor Haruyuki Atomi, Kyoto University

Copyright © 2021 American Society for Microbiology. All Rights Reserved.

Address correspondence to Delin You, dlyou@sjtu.edu.cn.

Received 24 January 2021

Accepted 25 April 2021

Accepted manuscript posted online 30 April 2021

Published 25 June 2021

Natural products (NPs) are a powerful source of chemical defenders to survive in the ever-changing environments and ecosystems (1). The whole NP pool is comprised of countless natural compounds falling into different classes including polyketides (PKs) (2), nonribosomal peptides (NRPs) (3), ribosomally synthesized and posttranslationally modified peptides (RiPPs) (4), saccharides, terpenoids, isoprenoids, alkaloids, aminoglycosides, nucleosides, etc. Structural diversity and complexity of NPs not only contribute to the various biological or ecological activities but also benefit the motivations to develop medicinally important new drugs (5). The immense structural characteristics are introduced during the biosynthetic assembly (6). Typically, for most of the NPs, the biosynthetic assembly line mainly involves the construction of the basic scaffold and various postassembly modifications on the nascent scaffold. The modifications play important roles in rigidifying the molecule and fixing the three-dimensional conformation, introducing polar groups to increase the water solubility, revealing structural motifs and reactive sites indispensable for target inhibition, and appending oligosaccharides that bind to specific DNA sequences (6). Based on the tailoring enzyme chemistries, the modification reactions can be grouped into two broad categories: oxidative transformations and group transfer reactions (7). The group transfer reactions, like methylation, acylation, halogenation, and glycosylation, play important roles in diversifying the molecular structure (8–10) and improving the pharmacological properties and the molecular mechanism of action (5). Sometimes, the tailoring reaction was the rate-limiting factor in the NP biosynthesis, and the engineering of the modification bottlenecks would lead to an efficient process to the desired metabolites (11–13).

Anisomycin (compound 1) (Fig. 1A) has been isolated from *Streptomyces* sp. (14). As a member of the pyrrolidine alkaloid antibiotics, it exhibits diverse biological and pharmacologic activities (15). Owing to its reversible 60S ribosomal subunit binding possibly through the acyl group, compound 1 can block peptide bond formation and shows potent selective activity against pathogenic protozoa and fungi (16). At present, compound 1 is commercially available under the name flagecidin for the treatment of plant-pathogenic fungi. Moreover, compound 1 exhibits high antitumor activity *in vitro*, with 50% inhibitory concentration (IC_{50}) values in the nanomolar range (17), and it can be used in a synergistic fashion with a cyclin-dependent protein kinase inhibitor to kill carcinoma cells (18). It can be used as a tool in molecular biology to activate mitogen-activated protein kinase signaling pathways (19). Recently, as one of the important effective components in agricultural antibiotic 120 (a broad-spectrum pesticide composed of the mixed secondary metabolites of *Streptomyces hygroscopicus* subsp. *beijingensis*), compound 1 has been widely used for controlling crop diseases in China (20). Meanwhile, it can stimulate the growth of fruit and vegetables due to the plant growth-regulating activities (21).

The diverse biological activities and structural features of compound 1 have attracted the attention of many chemists and biologists. To date, three analogues (compounds 6 [also named deacetylanisomycin], 12, and 13 [Fig. 1A]) with different chain lengths of acyl groups have been isolated and tested for biological activities. Even with the successful chemical synthesis (18), the biosynthesis of compound 1 has remained an enigma for a long time. Fortunately, the biosynthetic gene cluster of compound 1 in *Streptomyces hygrospinosus* subsp. *beijingensis* has been cloned successfully by using a bioactivity-guided library screening approach in our lab (15). The biosynthetic machinery has been identified through systematic gene functional analysis, *in vivo* gene inactivation, *in vitro* biochemical assays, and detailed chemical analysis (Fig. 1A). The biosynthetic pathway of compound 1 was revealed, involving an unprecedented assembly route of the core benzylpyrrolidine scaffold catalyzed by AniN and two-round unexpected transamination and cryptic glycosylation catalyzed by AniQ and AniO (15), respectively. Interestingly, four pairs of glycosylated and unglycosylated counterparts (compounds 2/3, 4/4a, 5/5a, and 7/7a [Fig. 1A]) have been identified. Tailoring reactions catalyzed by α -glucosidases AniG, methyltransferase AniK, and even acetyltransferase AniI were proposed not to follow a particular sequence, except that

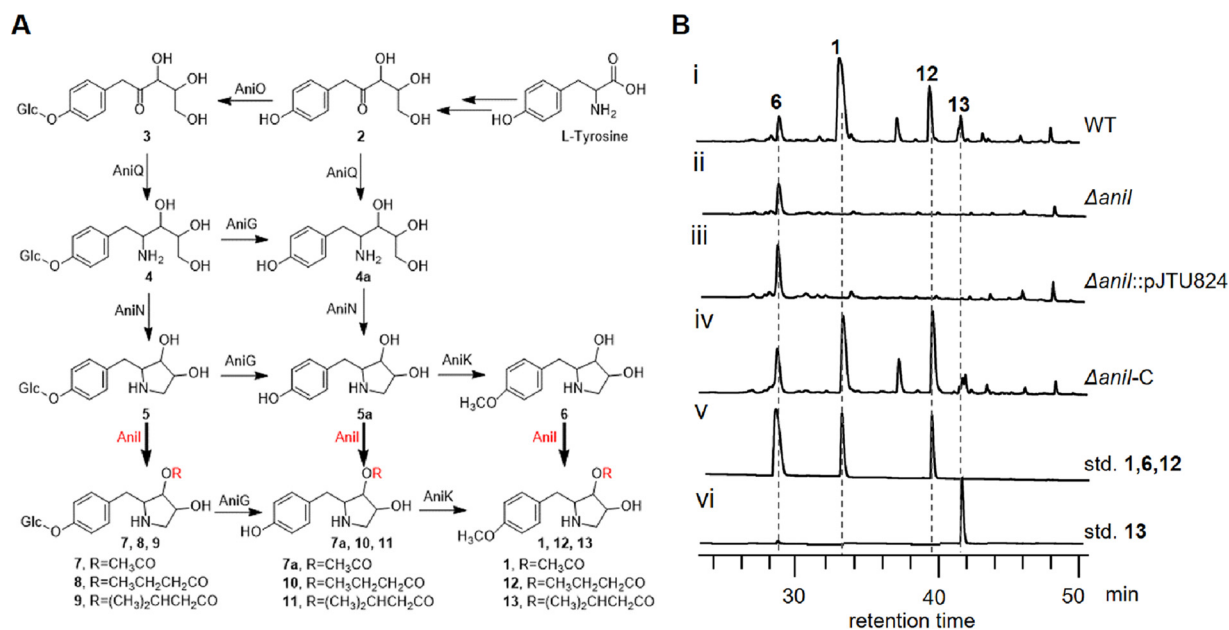


FIG 1 The biosynthetic pathway of compound 1 and complementation of *anil*. (A) The biosynthetic pathway of compound 1. The reactions catalyzed by Anil are highlighted in red. (B) The HPLC analysis of the fermentation products in genetic-interruption $\Delta anil$ strain (ii), complementary strain $\Delta anil$ -C (iv), the wild-type (WT) strain (i), and the control $\Delta anil$ -pJTU824 strain (iii). Standards 1, 6, and 12 (v) and standard 13 (vi) were used as controls.

deglycosylation must precede O-methylation on the phenol moiety. This likely accounts for the observation that the compound 1 producer strain is very “clean” (as no intermediates were accumulated in the wild-type [WT] strain), as the flexible enzymes can redirect shunt intermediates back into the pathway to compound 1. Actually, the tolerance of AniK and AniG has been demonstrated before (15). But, in the case of Anil, the possible flexibility and tolerance of different substrates still await discovery. Meanwhile, whether Anil could catalyze the transformation to compounds 12 and 13 is unknown (Fig. 1A).

The function of *anil* was characterized in this study. Anil exhibited tolerance of acyl group donors and acceptors, which might set the stage for efficient production of compounds 1, 12, and 13. Meanwhile, the activities of Anil toward synthesized compound 1 analogues provide a potential approach to construction of diverse pyrrolidine ring scaffolds in compound 1. Actually, the overexpression of *anil* contributed to the productivity improvement of compounds 1, 12, and 13. These findings reported here might supply good material for metabolic engineering of high-yield strains.

RESULTS

Anil was an indispensable acetyltransferase for compound 1, 12, and 13 biosynthesis. The previous genetic deletion of *anil* has completely abolished the production of compound 1 and resulted in the accumulation of compound 6 (Fig. 1B). Meanwhile, no accumulation of compounds 12 and 13 was detected (Fig. 1B). To exclude other possible explanations of the phenotype of the $\Delta anil$ mutant, a single copy of *anil* on the integrative plasmid pJTU824 was transferred into the $\Delta anil$ strain to construct the complementary strain $\Delta anil$ -C (see Fig. S1 in the supplemental material). The fermentation products of $\Delta anil$ -C were analyzed by liquid chromatography-mass spectrometry (LC-MS), and the production of compounds 1, 12, and 13 was restored (Fig. 1B), while the introduction of pJTU824 exhibited no effect on the biosynthesis of compound 6 (Fig. 1B). These data confirmed the indispensability of *anil* for biosynthesis of compound 1 and its derivatives (compounds 12 and 13) (Fig. 1B).

The *ani* gene cluster encoded an acetyltransferase with 222 amino acids (Anil, GenBank accession no. [ARE72418.1](https://www.ncbi.nlm.nih.gov/nuccore/ARE72418.1)), which belongs to the LbH-MAT-GAT sugar O-acetyltransferase

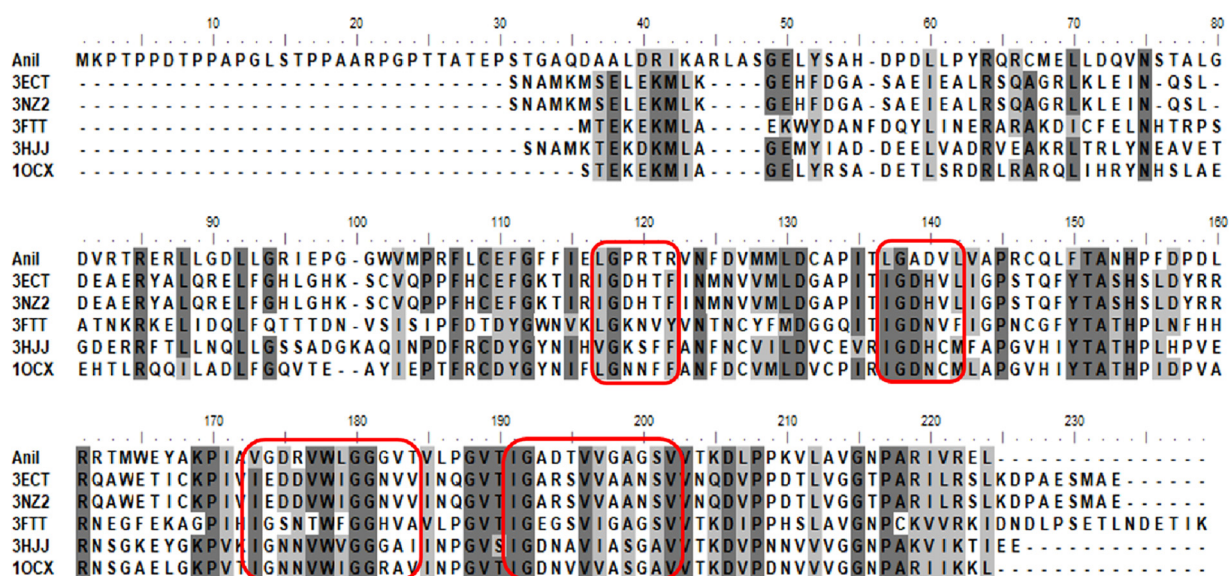


FIG 2 Multiple sequence alignment of Anil with LbH-MAT-GAT sugar O-acetyltransferase subfamily proteins. The “hexapeptide repeats” composed of typical ((LIV)-[GAED]-X-X-[STAV]-X) are marked with red rectangles.

(thiogalactoside transacetylase) subfamily (based on the NCBI BLASTP analysis). Maltose O-acetyltransferase (MAT) (like LacA [22] in *Escherichia coli*) acetylates maltose and glucose exclusively at the C-6 position of the nonreducing end glucosyl moiety. Galactoside O-acetyltransferase (GAT) specifically acetylates galactopyranosides. Active MAT and GAT are homotrimers, with each subunit consisting of an N-terminal alpha-helical region and a C-terminal left-handed parallel alpha-helix (LbH) subdomain with six turns, each containing three imperfect tandem repeats of a hexapeptide repeat motif ((LIV)-[GAED]-X-X-[STAV]-X) (23, 24). These repeating sequence motifs were termed “isoleucine patch” or “hexapeptide repeat” and have since been found as an easily identifiable and characteristic feature of this expanding family of acyltransferases (24). Anil showed 40% sequence identity with *E. coli* maltose acetyltransferase (PDB: 1OCX) (23) and 36% with maltose O-acetyltransferase (PDB: 3HJJ) from *Bacillus anthracis* and 37% with galactoside O-acetyltransferase (PDB: 3FTT) from *Staphylococcus aureus* (25). Moreover, a similar “hexapeptide repeat” can be found in Anil (Fig. 2). However, Anil exhibited no sequence identity with acetyltransferases reported in natural product biosynthesis like LovD (26), Bmml (27), 1,13-dihydroxy-*N*-methylcandine 13-O-acetyltransferase AT1 (28), and chloramphenicol acetyltransferase (CAT) (29). No member of the LbH-MAT-GAT sugar O-acetyltransferases has been found involved in natural product biosynthesis, and the lack of sequence identity with those acetyltransferases responsible for natural product biosynthesis suggested the different reaction site of Anil.

Anil exhibited broad substrate tolerance of biosynthetic intermediates. To verify that Anil was indeed responsible for the acylation modification reaction, we first cloned the intact *anil* gene into the pET28a plasmid for the construction of overexpressing plasmid pET28a-*anil* (Table 1) by one-step cloning using primers listed in Table 2. Then, the recombinant plasmid was transferred into *E. coli* BL21(DE3) for overexpression. The recombinant Anil was purified by nickel-nitrilotriacetic acid (Ni-NTA) affinity chromatography to near-homogeneity, and the purity and size (27.4 kDa) of resultant protein were determined by SDS-PAGE (Fig. S2).

For the biochemical demonstration on the acylation activity of Anil, we first conducted the *in vitro* enzymatic reaction with compound 6, which was accumulated in the $\Delta anil$ mutant. Acetyl coenzyme A (acetyl-CoA) was selected as the donor of the acetyl group, and the reaction system was composed of 500 μ M compound 6 and 20 μ M Anil and was incubated in phosphate-buffered saline (PBS) buffer at 30°C for 2 h. A new peak

TABLE 1 Strains and plasmids used in this study

Strain or plasmid	Description	Source or reference
Strains		
<i>Streptomyces</i> strains		
<i>S. hygrospinosus</i> subsp. <i>beijingensis</i>	Wild-type, anisomycin-producing strain	ACCC40033 (Agricultural Culture Collection of China)
$\Delta anil$	<i>anil</i> deletion mutant	15
$\Delta anil$ -C	<i>anil</i> -complementary mutant	This study
$\Delta anil::pJTU824$	Control strain of $\Delta anil$ -C	This study
WT::pOST- <i>anil</i>	<i>anil</i> overexpression strain under the control of the <i>kasOp</i> * promoter	This study
WT::pIB139- <i>anil</i>	<i>anil</i> overexpression strain under the control of the <i>ermE</i> * promoter	This study
WT::pOST	Control strain of WT::pOST- <i>anil</i>	This study
WT::pIB139	Control strain of WT::pIB139- <i>anil</i>	This study
<i>E. coli</i> strains		
DH10B	General molecule cloning strain	Gibco BRL
BL21(DE3)	Host for protein expression	Stratagene
ET12567/pUZ8002	Intergeneric conjugation strain	44
Plasmids		
pJTU824	Integrating vector containing <i>ermE</i> * promoter	45
pJTU824- <i>anil</i>	Derivate plasmid of pJTU824 with intact gene <i>anil</i> under the control of the <i>ermE</i> * promoter and used for complementation	This study
pET28a	Protein expression vector	Novagen
pET28a- <i>anil</i>	Derivate pET28a plasmid containing the intact gene <i>anil</i>	This study
pSET152	Integrative plasmid used for overexpression	46
pOST	Derived from pSET152 containing <i>kasOp</i> * promoter	This study
pOST- <i>anil</i>	Derivate plasmid of pOST with intact gene <i>anil</i> under the control of the <i>kasOp</i> * promoter and used for overexpression	This study
pIB139	Derived from pSET152 containing <i>ermE</i> * promoter	47
pIB139- <i>anil</i>	Derivate plasmid of pSET152 with intact gene <i>anil</i> under the control of the <i>ermE</i> * promoter and used for overexpression	This study

could be detected in the reaction system of Anil (Fig. 3), indicating that Anil is capable of acetylation. The retention time and mass value (Fig. 3) of the reaction product are consistent with the standard compound 1 (m/z 266.3, $[M+H]^+$). Using compound 1 as control, the tandem mass spectrometry (MS/MS) analysis of the acylated products was conducted, which showed the same fragmentation mode and suggested the loading of acetyl group to the hydroxyl group at C-3 on the pyrrolidine ring (Fig. S3). Thus, these data confirmed that Anil is responsible for the transformation of compound 6 into compound 1 (Fig. 1A). Meanwhile, the kinetics analysis showed that the k_{cat} value of Anil for compound 6 was 924 min^{-1} and the k_{cat}/K_m was $1.39 \mu\text{M}^{-1} \text{ min}^{-1}$ (Table 3 and Fig. S5).

Based on the proposed complex network of compound 1 biosynthesis, Anil possibly catalyzed the acetylation of other biosynthetic intermediates besides compound 6. To learn about the substrate scope of Anil, other biosynthetic intermediates such as compounds 2/3, 4/4a, and 5/5a were also used as the substrates within the acetylation reaction system supplied with acetyl-CoA (Fig. 3). Anil could not catalyze the acetylation of compounds 4/4a and 2/3, but it could acetylate compounds 5 and 5a into the corresponding acetylation product compounds 7 and 7a (Fig. 3), respectively, the MS values of which were confirmed by LC-MS analysis (Fig. S4). The loading of the acetyl group to the hydroxyl group at C-3 on the pyrrolidine ring was further confirmed by MS/MS analysis of products 7 and 7a (Fig. S3). So, Anil exhibited broad substrate specificity toward biosynthetic intermediates, which is consistent with other reported acyltransferases like LovD (26). Steady-state kinetic parameters were also determined for the acetylation of compounds 5 and 5a, and the K_m value of Anil for compounds 5 and 5a was $969.6 \mu\text{M}$ and $1,432 \mu\text{M}$, respectively. The k_{cat}/K_m for compound 5 ($1.93 \mu\text{M}^{-1} \text{ min}^{-1}$) was similar to

TABLE 2 Primers used in this study

Primer	Sequence (5'–3')	Use(s)
824-I-fw	GTTGGTAGGATCCACATATGATGAAACCGACGCCCCCGA (NdeI site)	Complementation of $\Delta anil$
824-I-rv	TATGACATGATTACGAATTCTCACAGCTCCCGGACGATGC (EcoRI site)	
thioF	ATGCGGGGATCGACCCGCGG	Validation of $\Delta anil$ -C
thioR	TCATCAGCTGCATACCGCTG	
I-A	AGCAAATGGGTCGCGGATCCATGAAACCGACGCCCCCGA (BamHI site)	Overexpression of His-tagged Anil protein in <i>E. coli</i>
I-S	TGTCGACGGAGCTCGAATTCTCACAGCTCCCGGACGATGC (EcoRI site)	
pSET152-pkasOp-F	GGGTCGAGGTCGACTCTAGATGTTTCACATTCGAACGGTCTCTG (XbaI site)	Overexpression of <i>anil</i> in WT strain
pSET152-pkasOp-R	CGCGCCCGGATCCTCTAGACTCCCCAGTCTGCACG (XbaI site)	
pSET152-Anil-F	TGGGGGAGTCTAGAGGATCCATGAAACCGACGCCCCCGA (BamHI site)	Overexpression of <i>anil</i> in WT strain
pSET152-Anil-R	TCGATATCGCGCGCGCCGCATATGTACAGCTCCCGGACGATGC (NotI site)	
pB139-Anil-F	GTTGGTAGGATCCACATATGATGAAACCGACGCCCCCGA (NdeI site)	Overexpression of <i>anil</i> in WT strain
pB139-Anil-R	CGCGCCCGGATCCTCTAGATCACAGCTCCCGGACGATGC (XbaI site)	
16S-RT-F	CCGCAAGGCTAAAACCTCAA	Detection of the transcriptional level of 16S rRNA
16S-RT-R	AACCAACATCTCACGACAC	
Anil-RT-F	CCCCGCTTCTGTGCGAGTT	Detection of the transcriptional level of <i>anil</i>
Anil-RT-R	GGTGGTTGGCGGTGAAGAGC	

that of compound 6, the value of which was triple that for compound 5a (Table 3 and Fig. S5). Based on the comparison, compound 5 seemed to be the preferred substrate of Anil when the acetyl group was used as acyl donor.

The promiscuity of Anil on acyl donors contributed to compound 12 and 13 production. From the results mentioned above, Anil could catalyze the transfer of the acetyl group to the hydroxyl group in the pyrrolidine ring of compound 1. Considering that the presence of the other two derivatives (compounds 12 and 13) accumulated in the WT strain, the butyryl group and isovaleryl group were proposed to be transferred onto the same hydroxyl group of compound 6 for compound 12 and 13 production, respectively. To verify the proposal, butyryl-CoA and isovaleryl-CoA were used as acyl group donors, respectively, in the *in vitro* reaction system of compound 6. As can be seen from Fig. 4A, the butyryl group and isovaleryl group could actually be recognized by Anil, and compounds 12 and 13 were indeed produced based on the MS/MS analysis (Fig. S3).

The broad substrate specificity toward the acyl donors and the acyl receptors was common for acyltransferase (26, 27). To further characterize the substrate tolerance of Anil, compounds 5 and 5a were used as the acceptors again for the butyryl group and isovaleryl group donated by butyryl-CoA and isovaleryl-CoA, respectively. The results depicted in Fig. 4B showed that Anil could catalyze the total transformation of compound 5 into the butyrylated and isovalerylated products 8 and 9, respectively. But only partial compound 5a was transformed into butyrylated and isovalerylated products 10 and 11, respectively. The MS and MS/MS value analysis of compounds 8, 9, 10, and 11 confirmed the successful loading of the butyryl and isovaleryl groups (Fig. S3 and S4). The results mentioned above showed that compound 5 was the preferred acyl acceptor. To compare the preferences on the acyl donors, compound 5 was selected and incubated with three kinds of acyl donors (acetyl-CoA, isovaleryl-CoA, and butyryl-CoA), respectively. The reaction was quenched at 10 min with the addition of an equal volume of chloroform. As shown in Table 3, the K_m values of Anil for three kinds of acyl group donors were similar, and the k_{cat}/K_m values for acetyl-CoA ($0.24 \mu\text{M}^{-1} \text{min}^{-1}$) and butyryl-CoA ($0.28 \mu\text{M}^{-1} \text{min}^{-1}$) were similar, too. However, the k_{cat}/K_m for isovaleryl-CoA ($\mu\text{M}^{-1} \text{min}^{-1}$) was half of them (Table 3 and Fig. S5). Taken together, all these results demonstrated the promiscuity of Anil for different donors and acceptors of different acyl groups.

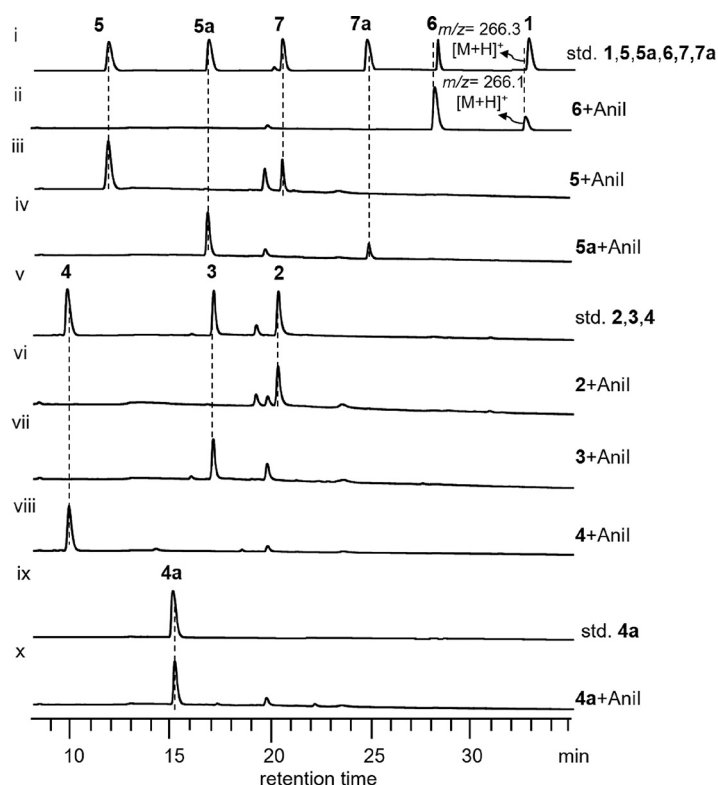


FIG 3 The acetylation reactions catalyzed by Anil. HPLC profile of reaction products catalyzed by Anil with compounds 6 (ii), 5 (iii), 5a (iv), 2 (vi), 3 (vii), 4 (viii), and 4a (x). The standard compounds 1, 5, 5a, 6, 7, and 7a (i); 2, 3, and 4 (v); and 4a (ix) were used as controls.

The acetylation was essential for the biological activity. It has been reported that the isotopically labeled compound 1 binds yeast and human tonsil ribosomes (30). Especially, the acetyl group at the C-3 position of the pyrrolidine ring in compound 1 was important for the ribosome interaction, since compound 6 showed 350-times-lower affinity for the ribosome (30). To determine the important role the acyl group plays in biological activity, we performed *in vitro* antifungal activity assays of compounds 6, 1, 12, and 13 (Fig. 5A). All the tested compounds other than compound 6 showed activity against *Saccharomyces sakei*. Particularly, according to the relative activities, these active compounds can be ordered as compound 1 > compound 12 > compound 13. Meanwhile, the loading of the acetyl group to compound 5a endowed it with similar antifungal activity (Fig. 5B). Consistently, the acetylated product 7a exhibited the strongest activity and the butyrylated product 11 showed the weakest activity. However, the acylation of compound 5 did not result in any antifungal activity (Fig. 5C), which suggested that the glycosylation may negatively affect the biological activity. These data indicated that the acylation was indispensable for antifungal bioactivities of compound 1 and its derivatives.

Overexpression of *anil* contributed to high productivities of compound 1 and its analogues. Tailoring reactions contribute to the structural diversity and play a vital

TABLE 3 A kinetics comparison of Anil with different acyl group donors and acceptors

Substrate 1	Substrate 2	K_m (μM)	k_{cat} (min^{-1})	k_{cat}/K_m ($\mu\text{M}^{-1} \text{min}^{-1}$)
Compound 6	Acetyl-CoA	664.50 ± 123.70	924.00 ± 63.08	1.39 ± 0.51
Compound 5	Acetyl-CoA	969.60 ± 372.90	$1,869.80 \pm 242.20$	1.93 ± 0.65
Compound 5a	Acetyl-CoA	$1,432.00 \pm 561.60$	644.40 ± 94.88	0.45 ± 0.17
Acetyl-CoA	Compound 5	666.10 ± 86.62	161.90 ± 6.44	0.24 ± 0.07
Butyryl-CoA	Compound 5	532.20 ± 117.10	150.10 ± 9.59	0.28 ± 0.08
Isovaleryl-CoA	Compound 5	517.50 ± 108.66	52.85 ± 5.40	0.10 ± 0.05

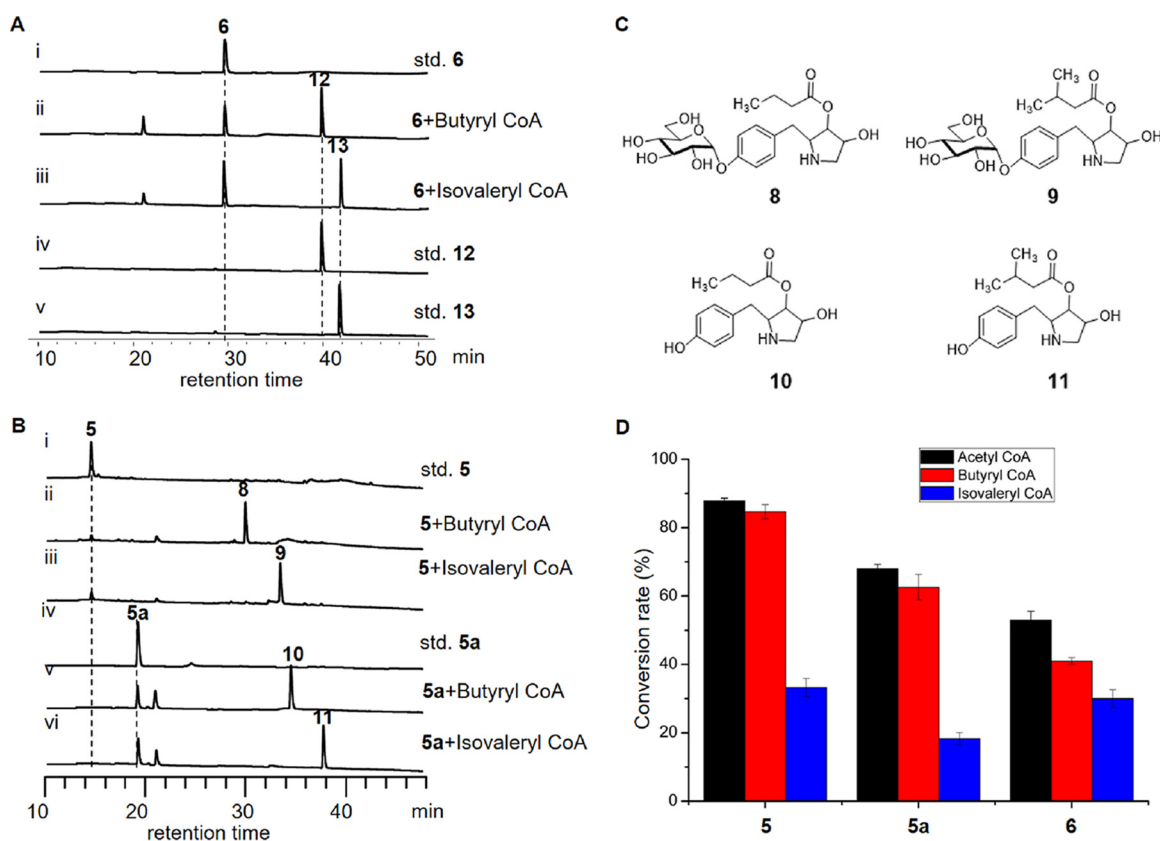


FIG 4 The characterization of substrate tolerance of Anil on acyl donors and acceptors. (A) HPLC profile of reaction products catalyzed by Anil with compound 6 with butyryl-CoA (ii) and isovaleryl-CoA (iii) group. Standards 12 and 13 were used as control. (B) Reactions of compounds 5 and 5a with butyryl-CoA (ii and v) and isovaleryl-CoA (iii and vi). Standards 5 (i) and 5a (iv) were used as control. (C) Molecular structures of compounds 8, 9, 10, and 11. (D) Comparative acylation activities analysis of compound 5, 5a, and 6 reaction with acetyl-CoA, butyryl-CoA, and isovaleryl-CoA. Typical 100- μ l reaction systems of 20 μ M Anil, 500 μ M compounds (5, 5a, and 6, respectively), and 1 mM acyl donors (acetyl-CoA, butyryl-CoA, and isovaleryl-CoA, respectively) in PBS buffer were incubated at 30°C for 30 min.

role in the maturation of desired compounds. Engineering of the modification bottlenecks would lead to an efficient process to the desired metabolites, and the overexpression of tailoring genes (such as genes for hydroxylase [11], O-methyltransferase [31], and halogenase [13]) has been reported to produce remarkable improvement in purity and productivity of desired products. According to the metabolic profile of the WT strain, compound 6 could not be transformed into the active acylated products *in vivo* completely (Fig. 1B). To promote the active acylated product transformation, the gene *anil* was cloned into the integrative vector pIB139 under the control of *permE** (Fig. 6A) and introduced into the WT strain through conjugation. Quantitative real-time reverse transcription-PCR (RT-qPCR) confirmed that *anil* was overexpressed in the recombinant strains (WT::pIB139-*anil*), and its transcription reached the highest level of 14.5-fold over that of the WT strain at 48 h (Fig. 6B). During the monitoring process, compound 1 was found to undergo deacetylation spontaneously in water (Fig. S6). That means that during the fermentation and detection process, the spontaneous inevitably occurs. So, the total production levels of compound 1 and its analogues (compounds 6, 12, and 13) were compared by high-pressure liquid chromatography (HPLC) analysis (Fig. 6C). As can be seen from Fig. 6D, the production of those four compounds was decreased slightly in the WT::pIB139 strain, suggesting a negative effect of the pIB139 integration. Fortunately, deducting the negative effect of empty plasmid, the productivity increased obviously and was 2.69 times that in the WT::pIB139-*anil* strain (Fig. 6D). Considering that the efficiency of promoter might be a limiting factor, we also tried another potent

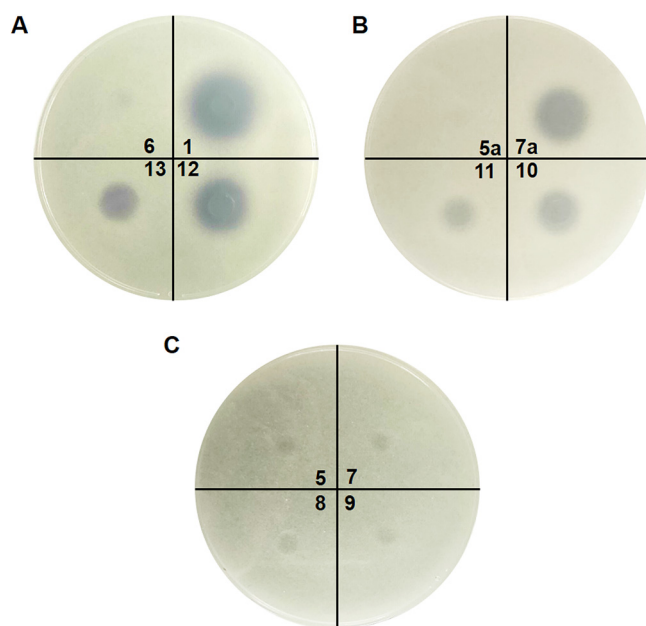


FIG 5 Bioactivity assay of compounds 6, 1, 12, and 13 (A); 5a, 7a, 10, and 11 (B); and 5, 7, 8, and 9 (C) used in this study. All the tested compounds were dissolved in water with the final concentration of 1 mM, 30 μ l of which was used for assay.

promoter, *pkasO**, and constructed the plasmid pOST, by integrating *pkasO** into pSET152 (Fig. 6A). Then, a copy of intact *anil* was introduced into this plasmid, and the resultant pOST-*anil* was then transferred into the WT strain. Similarly, the transcription of *anil* was also increased in the resultant overexpressing strain, about 11-fold that observed in the WT strain (Fig. 6B). Meanwhile, plasmid pOST exerted a negative effect on compound accumulation and the production was increased in the WT::pOST-*anil* strain (about 2.03-fold that in the WT::pOST strain) (Fig. 6D). These data showed that the overexpression of *anil* was an efficient way to improve the fermentation titers of anisomycin and its analogues. So, more efficient promoters should be tried for further productivity improvement in future.

DISCUSSION

The acylation of oxygen-containing substrates is one of the most common modification types of secondary metabolites. Acyl-sugars, acylated acyl carrier proteins, or acyl-activated coenzyme A thioesters can serve as activated acyl donors. Acetylation could increase the structural diversity and affect the chemical stability, volatility, biological activity, and even the cellular localization of specialized compounds (32). During the biosynthesis of NPs, the loaded acetyl group could serve as a stabilizing group that prevents ring opening and facilitates subsequent reactions (33), as the protective group makes the biosynthesis a unique and highly ordered process (28) and mediates the transport of biosynthetic intermediates (34). Recently, acetylation has also been reported for the condensation of the polyketide and ribosomally synthesized and posttranslationally modified peptides RiPP moieties (PK/RiPPs) involved in goadionin biosynthesis (35).

Little is known about the acylation of anisomycin. In this study, the complementation of an intact *anil* gene into the Δ *anil* mutant successfully restored the production of compounds 1, 12, and 13, suggesting the indispensability of this gene (Fig. 1B). To verify the acyl group transferring activity, compound 6 and acetyl-CoA were first used as the substrates for Anil, and compound 6 could be transformed to compound 1 (Fig. 3). These data confirmed that Anil acted on the pyrrolidine ring, which was different from the typical reported sites on sugar targets of the LbH-MAT-GAT sugar O-acetyltransferase

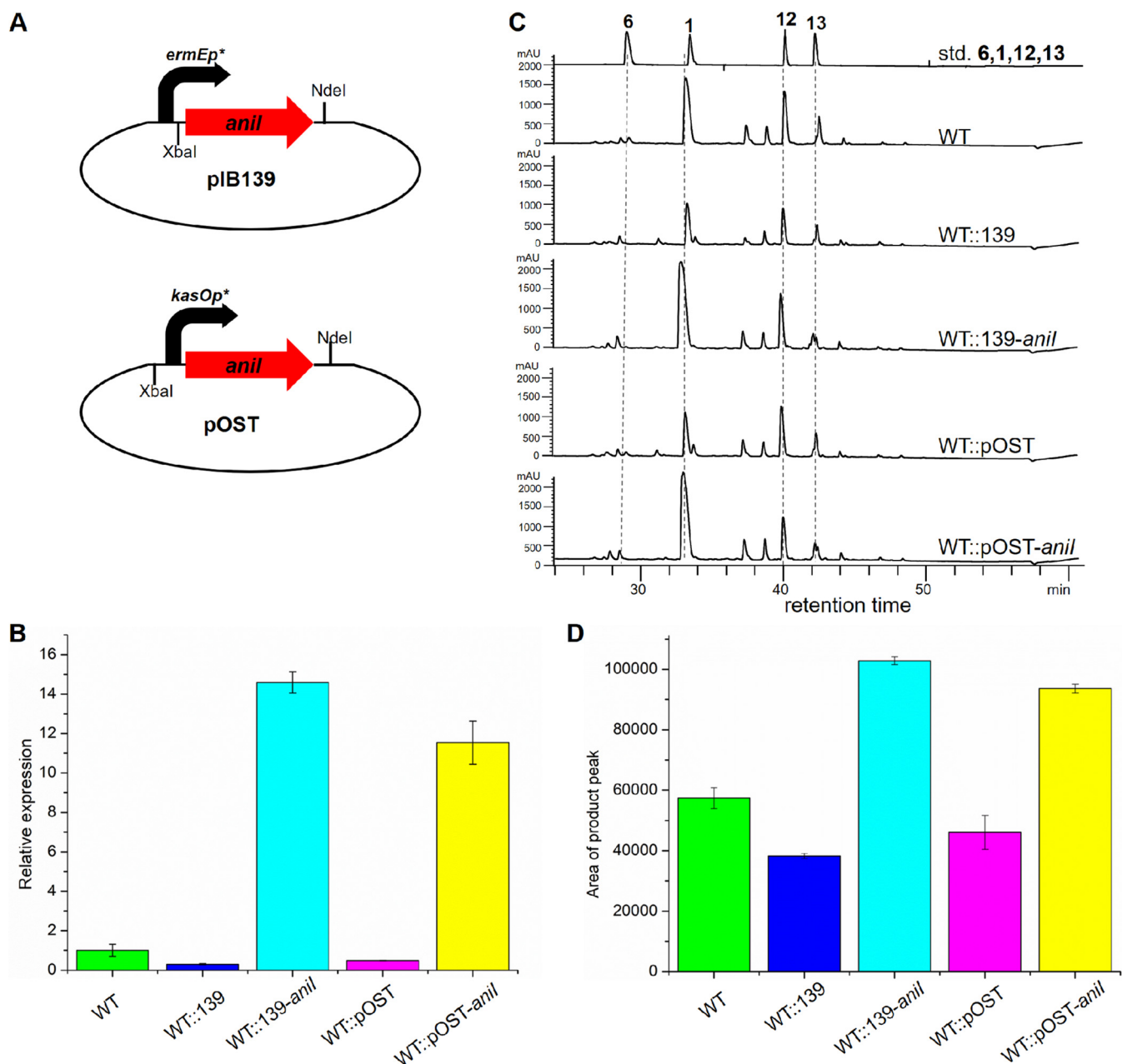


FIG 6 The construction and characterization of *anil*-overexpressing strains. (A) The depiction of construction of *anil* overexpression plasmids using pIB139 and pOST. (B) The RT-qPCR analysis of the transcription of *anil* in the WT::pIB139-*anil* and WT::pOST-*anil* strains. (C) The HPLC analysis of the products accumulated in different strains. The standard compounds 1, 6, 12, and 13 were used as controls. (D) The productivity analysis of compound 1 and its analogues in the overexpressing strains.

subfamily (Fig. 2). Considering the complex biosynthetic network of compound 1 (Fig. 1A), the biosynthetic intermediates 2/3, 4/4a, and 5/5a were also tested as the substrates for Anil. Only compounds 5 and 5a could be acetylated (Fig. 3), suggesting the necessity of the pyrrolidine ring. The catalytic efficiency (k_{cat}/K_m) of compound 5 was about 4.5-fold that of compound 5a (Table 3). To test the promiscuity of Anil on the structure of the pyrrolidine ring, analogues with different modifications of the pyrrolidine ring were prepared. The -OH group at C-4 of the pyrrolidine ring was modified with a methyl and benzyl group in analogues 15 and 17, respectively (see Fig. S7 and S8 in the supplemental material). Then, compounds 15 and 17 were separately used as the substrate for Anil, and the acetyl group was successfully loaded onto the C-3-OH (Fig. S9), which confirmed the promiscuity of Anil on the structure of the pyrrolidine ring. These data suggested that

Anil might be developed by protein engineering for biocatalytic synthesis of pyrrolidine rings with diverse modifications.

Moreover, Anil showed promiscuity of other acyl donors, such as the butyryl-CoA group and isovaleryl-CoA, and even the acetylated biosynthetic intermediates like compound 7 (Fig. S10). When the butyryl-CoA group and isovaleryl-CoA were used as acyl donor for compound 6, Anil could catalyze the transformation of compounds 6 to 12 and 13, respectively (Fig. 4A). The conversion rate suggested the preference of Anil on acyl donors, and the preference could be ordered as acetyl-CoA > butyryl-CoA > isovaleryl-CoA. When biosynthetic intermediates 5 and 5a were used as acceptors for butyryl and isovaleryl groups, respectively, the conversion rates of compound 5 to acylated products 8 and 9 were obviously higher than that of compounds 5a to 10 and 11 (Fig. 4D). Consistently, using compound 5 as the acceptor, Anil exhibited similar reaction efficiencies toward acetyl-CoA (k_{cat}/K_m of $0.24 \mu\text{M}^{-1} \text{min}^{-1}$) and butyryl-CoA (k_{cat}/K_m of $0.28 \mu\text{M}^{-1} \text{min}^{-1}$) and showed relatively low activity on isovaleryl-CoA (k_{cat}/K_m of $0.1 \mu\text{M}^{-1} \text{min}^{-1}$). Moreover, acetylated compound 7 was found to act as acetyl donor and was transformed into deacetylated compound 5, resulting in the formation of acetyl-CoA (Fig. S10A). So, Anil catalyzed the reversible interconversion of acetylated compound 7 and acetyl-CoA (Fig. S10B). Taken together, Anil exhibited promiscuity of acyl donors and acceptors but showed preference simultaneously. However, more acyl donors should be tested in future for biocatalyst development.

Additionally, the acylation of compounds 5a and 6 turned out to be essential for the antifungal activity. Interestingly, the loading of the acetyl group gave the corresponding product (compounds 7a and 1) higher activity (Fig. 5A and B). These results proved the indispensability of the acyl group for the biological activities, which was consistent with the previously identified importance of the acetyl group for the ribosome binding activity. However, none of the acylated products of compound 5 (namely, compounds 7, 8, and 9) was active against *Saccharomyces sakei* (Fig. 5C), which reflected the necessity of the glycosyl group removal catalyzed by AniG.

The existence of compound 6 suggested that the activity of Anil might be the bottleneck for higher productivities of compound 1. To give further support for this hypothesis, the *anil*-overexpressing strain *anil*-C was constructed (Fig. 6A), and fortunately, the total productivities of compound 1 and its analogues were obviously improved in the overexpressing strains (Fig. 6D). This finding served as another successful exploration of tailoring gene engineering for productivity improvement of desired metabolites (13, 18–20).

In summary, this study highlighted the indispensable roles of *anil* for the biosynthesis of compound 1 and its derivatives. Anil was found to be a typical acyltransferase with high promiscuity toward various acyl group donors and acceptors. Findings reported here may improve the biosynthetic understanding of compound 1 and suggest that Anil could be developed for the construction of more complex pyrrolidine ring scaffolds in compound 1, which would have important implications to researchers in both the biosynthesis and chemical synthesis fields.

MATERIALS AND METHODS

Strains, plasmids, and general techniques for DNA manipulations. Bacterial strains and plasmids used in this study are listed in Table 1. Primers used for plasmid construction are listed in Table 2. General procedures for *E. coli* or *Streptomyces* manipulation were carried out according to the standard procedure (36, 37). For expression of *anil*, a 669-bp DNA fragment carrying the intact *anil* (669 bp) and two 20-bp homologous arms were amplified by PCR with primers I-A and I-S (listed in Table 2). The two homologous arms carried the sequence of the upstream region containing the BamHI site and the downstream region containing the EcoRI site, respectively. The PCR product was cloned into the BamHI/EcoRI-digested pET28a, generating the recombinant *anil* expression vector *anil*-pET28a, using the Ezmax one-step cloning kit (Tolo Biotech, China) (38). To construct the plasmid for the complementary strain (Δ *anil*-C) of the Δ *anil* mutant, fragments digested by NdeI and EcoRI were ligated into pJTU824 for the construction of *anil*-complementary vector pJTU824-*anil*. The resultant plasmid was first transferred into *E. coli* ET12567/pUZ8002 and then introduced into the Δ *anil* strain for the construction of complementary strain Δ *anil*-C. The fermentation of Δ *anil*, Δ *anil*-C, and wild-type (WT) strains was conducted according to the protocol described before (39, 40). The *kasOp** was cloned into the XbaI-digested integrative

plasmid pSET152 for the construction of pOST, using the primers pSET152-pkasOp-F/R (Table 2). Subsequently, fragments of *anil* with flanking restriction sites of BamHI/NotI were amplified using corresponding primers (Table 2) and successively cloned into pOST-*kasOp** to generate pOST-*anil*. Similarly, fragments of *anil* with restriction sites of NdeI/NotI were amplified using corresponding primers (Table 2) and then inserted into pIB139 to generate pIB139-*anil*. The recombinant plasmids were introduced into the Δ *anil* strain or *S. hygrospinosus* subsp. *beijingensis* via intergeneric conjugation. The double-crossover strains were obtained through antibiotic selection and confirmed by PCR verification.

Bioinformatics analysis. The bioinformatics analysis of Anil was conducted with the online software NCBI BLASTP (<https://blast.ncbi.nlm.nih.gov/>). Multiple sequences were aligned using ClustalW (41). Proteins used for sequence alignment are as follows: maltose O-acetyltransferase (PDB: 1OCX) from *E. coli*, maltose O-acetyltransferase (PDB: 3HJJ) from *Bacillus anthracis*, galactoside O-acetyltransferase (PDB: 3FTT) from *Staphylococcus aureus*, hexapeptide-repeat-containing acetyltransferase VCA0836 (PDB: 3NZ2) from *Vibrio cholerae* O1 biovar eltor, and hexapeptide-repeat-containing acetyltransferase (PDB: 3ECT) from *Vibrio cholerae*.

Protein expression and purification. The expression plasmids for Anil were transformed into *E. coli* BL21(DE3)/pLysE. The resultant *E. coli* BL21 cell was cultured at 37°C and 220 rpm on a shaking incubator in Luria-Bertani (LB) medium supplemented with kanamycin at the final concentration of 50 μ g/ml to an optical density at 600 nm (OD_{600}) of 0.6. Isopropyl- β -D-thiogalactoside (IPTG) with an 0.2 mM final concentration was added into the culture after cooling at 4°C for 30 min to induce protein expression. The cells were further cultured at 16°C for 24 h. Then, the cells were harvested by centrifugation (1,500 \times g, 15 min, 4°C), resuspended in 20 ml buffer A (50 mM Tris-HCl, pH 8.0, 0.3 M NaCl, and 10% glycerol), and lysed by sonication for 40 min. Cellular debris was removed by centrifugation (6,500 \times g, 60 min, 4°C), and the supernatant was used to purify the protein by nickel-affinity chromatography using standard protocols. The protein was eluted with an increasing gradient of buffer B (500 mM imidazole in buffer A). Eluted proteins were concentrated with the centrifugal filters (Amicon) (10 kDa), desalted using a PD-10 desalting column (GE Healthcare), and finally exchanged into buffer (50 mM Tris-HCl, 30 mM NaCl, pH 8.0). The protein was stored in 150 mM NaCl, 50 mM Tris-HCl (pH 8.0) buffer with 10% glycerol at -80°C . Protein concentration was determined with the Bradford assay using bovine serum albumin as a standard.

Enzyme assays. A typical 100- μ l system consists of 500 μ M acetyl-CoA, 500 μ M compounds. The reactions were initiated by the addition of Anil (the final concentration was 20 μ M), and the reaction mixtures were then incubated for 2 h at 30°C. Reaction mixtures were quenched by addition of an equal volume of water and then extracted by an equal volume of chloroform three times. The reaction system was first centrifuged, and then the resultant supernatant was concentrated to dryness and finally was dissolved in 40 μ l double-distilled water (ddH_2O) before HPLC analysis.

The resultant product was analyzed by an Agilent HPLC series 1100 with an Agilent Zorbax SB-C₁₈ column (5 μ m, 4.6 by 250 mm). The column was equilibrated with 95% (vol/vol) solvent A (H_2O with 0.1% [vol/vol] trifluoroacetic acid) and 5% (vol/vol) solvent B (acetonitrile), developed with a linear gradient (5 to 30 min, from 5% B to 50% B, 30 to 45 min, from 50% B to 95% B), and then kept at 95% B for 5 min at a flow rate of 0.5 ml/min and UV detection at 223 nm. LC-MS analysis was conducted with an Agilent 1100 series LC/MSD trap system with drying gas flow of 10 ml/min, nebulizer of 30 lb/in², and drying gas temperature of 350°C. For high-resolution mass measurements of the reaction products, an Agilent 1200 series LC/MSD trap system in tandem with a 6530 accurate-mass quadrupole time of flight (Q-TOF) mass spectrometer was used with an electrospray ionization (ESI) source (100 to 1,000 m/z mass range, positive mode).

Kinetics characterizations. To measure the k_{cat} and K_m for the acylation, we set up a series of 100- μ l reaction systems containing 50 to 3,200 μ M compound 5 (compounds 5a and 6) with the supply with 6 mM acetyl-CoA in PBS buffer (pH 8.0). For the comparison of kinetics parameters of Anil on different acyl groups, 1 to 3 mM compound 5 was used as the substrate incubated with 50 to 3,200 or 50 to 6,400 μ M acetyl-CoA, butyryl-CoA group, and isovaleryl-CoA, respectively. All the reaction components were mixed thoroughly, and 0.1 μ M Anil was added to initiate the reaction. Reactions were quenched at 10 min, 20 min, and 30 min (as Anil could catalyze the reverse reaction) by addition of an equal volume of water and then extracted by an equal volume of chloroform. After extraction three times, the water layer was combined and concentrated to dryness, which finally was dissolved in water before HPLC analysis. Reactions were run in triplicate, and the steady-state parameters k_{cat} and K_m were determined by nonlinear fitting of the Michaelis-Menten equation using GraphPad Prism 5.

Bioactivity determination of compound 1 and its derivatives. *Saccharomyces sakei* was inoculated into YEME medium (yeast extract, 3 g/liter; tryptone, 5 g/liter; maltose, 3 g/liter; glucose, 10 g/liter; sucrose, 103 g/liter) and incubated at 30°C for 24 h before use. One-milliliter cultures were harvested by centrifugation and resuspended in residual liquid. The suspended bacterial liquid was added to 20 ml molten potato dextrose agar (PDA) medium, cooled to about 55°C, mixed immediately, and poured into the plate. The Oxford cup was placed at the marked position and dipped slightly into the medium after the plate was dry. The corresponding compounds were added to the Oxford cup and then incubated at 30°C for 24 h for observation.

Transcriptional analysis of *anil* by real-time RT-qPCR. The fermentation cultures of WT and *anil* overexpression mutant strains were collected at 48 h separately. Total RNA was extracted from the mycelia using Redzol reagent according to the manufacturer's protocol (SBS Genetech Co., Ltd.). To exclude the interference by genomic DNA (gDNA), RNA extractions were digested with gDNA wiper (Vazyme Biotech Co., Ltd.). A 1- μ g RNA sample was reverse transcribed with HiScript III qRT SuperMix (Vazyme Biotech Co., Ltd.) according to the manufacturer's instructions. The transcriptional levels of *anil* were determined by real-time RT-qPCR using an ABI 7500 with ChamQ universal SYBR qPCR master mix (Vazyme Biotech Co., Ltd.). A two-step cycling protocol was used with uracil-DNA glycosylase

pretreatment at 50°C (2 min) and initial denaturation at 95°C (30 s) followed by 40 cycles of 95°C (30 s) and 60°C (30 s). The primers Anil-RT-F/R (listed in Table 2) were used for *anil* analysis. The *hrdB* gene encoding the major sigma factor in *Streptomyces* was used as the internal control.

Preparation and enzymatic assay of the analogues 15 and 17. For the preparation of compound 15, a 500- μ l reaction system composed of 5 mg compound 1, 2.11 mg *t*-BuOK, and 2.68 mg MeI was incubated at room temperature overnight, following the reported procedure (42). The reaction mixture was concentrated to dryness and then dissolved in methanol. The purification of compound 14 (the C-4-OH was methylated) was conducted with a semipreparative Agilent Zorbax SB-C₁₈ column (5 μ m, 9.4 by 250 mm). The column was equilibrated with 80% (vol/vol) solvent A (H₂O with 0.1% [vol/vol] trifluoroacetic acid) and 20% (vol/vol) solvent B (acetonitrile), developed with the isocratic elution for 25 min, and then kept at 100% B for 10 min at a flow rate of 1.5 ml/min and UV detection at 223 nm. The fraction with molecular weight 280.2 (*m/z*, [M+H]⁺) was determined by LC-MS analysis with an Agilent 1100 series LC/MSD trap system (drying gas flow, 10 ml/min; nebulizer, 30 lb/in²; and drying gas temperature, 350°C). The resultant compound 14 was dissolved in 1 ml methanol, and 200 μ l was isolated and added into the sodium hydroxide (10% [wt/vol])-methanol mixture for the deacetylation of the C-3-OH for the production of compound 15 (*m/z*=238.1, [M+H]⁺). The reaction system was centrifuged (13,000 \times *g*, 10 min) to obtain supernatant, which was then concentrated to dryness and then dissolved in water. After purification, the organic phase of the extraction by ethyl acetate was then dissolved in 200 μ l of methanol, which was used as stock solution of compound 15.

For the preparation of compound 17, a 500- μ l reaction system composed of 5 mg compound 1, 3.22 mg BnBr, and 4.37 mg Ag₂O dissolved in dimethylformamide (DMF) was incubated at room temperature for 48 h, according to methods previously reported (43). The reaction product 16 with a molecular weight of 356.2 (*m/z*, [M+H]⁺) was determined by LC-MS analysis and then purified by semipreparative HPLC (by isocratic elution of 40% B), using the same method described above. The deacetylation of compound 16 for the transformation to compound 17 was conducted similarly. The resultant purified compound 17 was dissolved in 200 μ l of methanol.

A typical 100- μ l system consists of 1 mM acetyl-CoA, and 4 μ l of compound 15 or 17 dissolved in PBS buffer (pH 8.0) was prepared for the enzymatic assay. The reactions were initiated by the addition of Anil with 20 μ M final concentration, and reaction mixtures were then incubated for 30 min at 30°C. Reaction mixtures were quenched by addition of 400 μ l methanol. The reaction system was first centrifuged, and then the resultant supernatant was concentrated to dryness, which finally was dissolved in 40 μ l ddH₂O before Q-TOF analysis. The Q-TOF analysis was conducted with an Agilent 1200 series LC/MSD trap system in tandem with a 6530 accurate-mass Q-TOF mass spectrometer. The ESI source (100 to 1,000 *m/z* mass range, positive mode) and collision energy of 50 V were used. The column was equilibrated with 95% (vol/vol) solvent A (H₂O with 0.1% [vol/vol] formic acid) and 5% (vol/vol) solvent B (acetonitrile) and developed with a linear gradient (5 to 30 min, from 5% B to 50% B; 30 to 40 min, from 50% B to 95% B) and then kept at 95% B for 5 min at a flow rate of 0.3 ml/min and UV detection at 223 nm and 280 nm.

SUPPLEMENTAL MATERIAL

Supplemental material is available online only.

SUPPLEMENTAL FILE 1, PDF file, 1.7 MB.

ACKNOWLEDGMENTS

This work was supported by grants from the National Key R&D Program of China (2018YFA0900400) from the Ministry of Science and Technology, the National Natural Science Foundation of China (31630002, 31700029, 31770038, and 21661140002), the Shanghai Pujiang Program from the Shanghai Municipal Council of Science and Technology (12PJD021), and the China Postdoctoral Science Foundation (2017M620151).

We declare that we have no conflicts of interest with the contents of this article.

Author contributions: Qing Wang and Lingxin Kong, investigation and methodology; Qing Wang, Xiaoqing Zheng, and Jufang Shen, data curation; Junbo Wang, Dashan Zhang, Yongjian Qiao, Jinjin Wang, and Zixin Deng, data analysis; Qing Wang and Lingxin Kong, writing—original draft; Lingxin Kong and Delin You, writing—review and editing.

REFERENCES

1. Zhang X, Li S. 2017. Expansion of chemical space for natural products by uncommon P450 reactions. *Nat Prod Rep* 34:1061–1089. <https://doi.org/10.1039/c7np00028f>.
2. Shen B. 2003. Polyketide biosynthesis beyond the type I, II and III polyketide synthase paradigms. *Curr Opin Chem Biol* 7:285–295. [https://doi.org/10.1016/S1367-5931\(03\)00020-6](https://doi.org/10.1016/S1367-5931(03)00020-6).
3. Walsh CT. 2016. Insights into the chemical logic and enzymatic machinery of NRPS assembly lines. *Nat Prod Rep* 33:127–135. <https://doi.org/10.1039/C5NP00035A>.
4. Hegemann JD, Zimmermann M, Xie X, Marahiel MA. 2015. Lasso peptides: an intriguing class of bacterial natural products. *Acc Chem Res* 48:1909–1919. <https://doi.org/10.1021/acs.accounts.5b00156>.
5. Tan GY, Liu T. 2017. Rational synthetic pathway refactoring of natural products biosynthesis in *Actinobacteria*. *Metab Eng* 39:228–236. <https://doi.org/10.1016/j.ymben.2016.12.006>.
6. Tang M-C, Zou Y, Watanabe K, Walsh CT, Tang Y. 2017. Oxidative cyclization in natural product biosynthesis. *Chem Rev* 117:5226–5333. <https://doi.org/10.1021/acs.chemrev.6b00478>.

7. Walsh CT, Fischbach MA. 2010. Natural products version 2.0: connecting genes to molecules. *J Am Chem Soc* 132:2469–2493. <https://doi.org/10.1021/ja909118a>.
8. Cabry MP, Offen WA, Saleh P, Li Y, Winzer T, Graham IA, Davies GJ. 2019. Structure of *Papaver somniferum* O-methyltransferase 1 reveals initiation of noscapine biosynthesis with implications for plant natural product methylation. *ACS Catal* 9:3840–3848. <https://doi.org/10.1021/acscatal.9b01038>.
9. Cho JH, Park Y, Ahn JH, Lim Y, Rhee S. 2008. Structural and functional insights into O-methyltransferase from *Bacillus cereus*. *J Mol Biol* 382:987–997. <https://doi.org/10.1016/j.jmb.2008.07.080>.
10. Rix U, Fischer C, Remsing LL, Rohr J. 2002. Modification of post-PKS tailoring steps through combinatorial biosynthesis. *Nat Prod Rep* 19:542–580. <https://doi.org/10.1039/b103920m>.
11. Chen Y, Deng W, Wu J, Qian J, Chu J, Zhuang Y, Zhang S, Liu W. 2008. Genetic modulation of the overexpression of tailoring genes *eryK* and *eryG* leading to the improvement of erythromycin A purity and production in *Saccharopolyspora erythraea* fermentation. *Appl Environ Microbiol* 74:1820–1828. <https://doi.org/10.1128/AEM.02770-07>.
12. Zhou X, Wu H, Li Z, Zhou X, Bai L, Deng Z. 2011. Over-expression of UDP-glucose pyrophosphorylase increases validamycin A but decreases validoxylamine A production in *Streptomyces hygroscopicus* var. *jinggangensis* 5008. *Metab Eng* 13:768–776. <https://doi.org/10.1016/j.jymben.2011.10.001>.
13. Zhu T, Cheng X, Liu Y, Deng Z, You D. 2013. Deciphering and engineering of the final step halogenase for improved chlortetracycline biosynthesis in industrial *Streptomyces aureofaciens*. *Metab Eng* 19:69–78. <https://doi.org/10.1016/j.jymben.2013.06.003>.
14. Sobin BA, Tanner FW. 1954. Anisomycin, a new anti-protozoan antibiotic. *J Am Chem Soc* 76:4053–4053. <https://doi.org/10.1021/ja01644a076>.
15. Zheng X, Cheng Q, Yao F, Wang X, Kong L, Cao B, Xu M, Lin S, Deng Z, Chooi Y-H, You D. 2017. Biosynthesis of the pyrrolidine protein synthesis inhibitor anisomycin involves novel gene ensemble and cryptic biosynthetic steps. *Proc Natl Acad Sci U S A* 114:4135–4140. <https://doi.org/10.1073/pnas.1701361114>.
16. Grollman AP. 1967. Inhibitors of protein biosynthesis: II. Mode of action of anisomycin. *J Biol Chem* 242:3226–3233. [https://doi.org/10.1016/S0021-9258\(18\)95953-3](https://doi.org/10.1016/S0021-9258(18)95953-3).
17. Hosoya Y, Kameyama T, Naganawa H, Okami Y, Takeuchi T. 1993. Anisomycin and new congeners active against human tumor cell lines. *J Antibiot* 46:1300–1302. <https://doi.org/10.7164/antibiotics.46.1300>.
18. Hulme AN, Rosser EM. 2002. An aldol-based approach to the synthesis of the antibiotic anisomycin. *Org Lett* 4:265–267. <https://doi.org/10.1021/ol017016u>.
19. Cano EDY, Ben-Levy R, Cohen P, Mahadevan LC. 1996. Identification of anisomycin-activated kinases p45 and p55 in murine cells as MAPKAP kinase-2. *Oncogene* 4:805–812.
20. Wang X, Ren Q. 1994. Analysis on the effective components of agricultural antibiotic 120. *Zhongguo Shengwu Fangzhi Xuebao* 10:131–134.
21. Yamada O, Kaise Y, Futatsuya F, Ishida S, Ito K, Yamamoto H, Munakata K. 1972. Studies on plant growth-regulating activities of anisomycin and toyocamycin. *Agric Biol Chem* 36:2013–2015. <https://doi.org/10.1271/bbb1961.36.2013>.
22. Wang XG, Olsen LR, Roderick SL. 2002. Structure of the *lac* operon galactoside acetyltransferase. *Structure* 10:581–588. [https://doi.org/10.1016/S0969-2126\(02\)00741-4](https://doi.org/10.1016/S0969-2126(02)00741-4).
23. Lo Leggio L, Dal Degan F, Poulsen P, Andersen SM, Larsen S. 2003. The structure and specificity of *Escherichia coli* maltose acetyltransferase give new insight into the LacA family of acyltransferases. *Biochemistry* 42:5225–5235. <https://doi.org/10.1021/bi0271446>.
24. Roderick SL. 2005. The *lac* operon galactoside acetyltransferase. *C R Biol* 328:568–575. <https://doi.org/10.1016/j.crv.2005.03.005>.
25. Luo HB, Knapik AA, Petkowski JJ, Demas M, Shumilin IA, Zheng H, Chruszcz M, Minor W. 2013. Biophysical analysis of the putative acetyltransferase SACOL2570 from methicillin-resistant *Staphylococcus aureus*. *J Struct Funct Genomics* 14:97–108. <https://doi.org/10.1007/s10969-013-9158-6>.
26. Xie X, Watanabe K, Wojcicki WA, Wang CC, Tang Y. 2006. Biosynthesis of lovastatin analogs with a broadly specific acyltransferase. *Chem Biol* 13:1161–1169. <https://doi.org/10.1016/j.chembiol.2006.09.008>.
27. Xiao F, Dong S, Liu Y, Feng Y, Li H, Yun CH, Cui Q, Li W. 2020. Structural basis of specificity for carboxyl-terminated acyl donors in a bacterial acyltransferase. *J Am Chem Soc* 142:16031–16038. <https://doi.org/10.1021/jacs.0c07331>.
28. Dang TT, Chen X, Facchini PJ. 2014. Acetylation serves as a protective group in noscapine biosynthesis in opium poppy. *Nat Chem Biol* 11:104–106. <https://doi.org/10.1038/nchembio.1717>.
29. Biswas T, Houghton JL, Garneau-Tsodikova S, Tsodikov OV. 2012. The structural basis for substrate versatility of chloramphenicol acetyltransferase CATI. *Protein Sci* 21:520–530. <https://doi.org/10.1002/pro.2036>.
30. Barbacid M, Vazquez D. 1974. [³H] anisomycin binding to eukaryotic ribosomes. *J Mol Biol* 84:603–623. [https://doi.org/10.1016/0022-2836\(74\)90119-3](https://doi.org/10.1016/0022-2836(74)90119-3).
31. Tan GY, Deng K, Liu X, Tao H, Chang Y, Chen J, Chen K, Sheng Z, Deng Z, Liu T. 2017. Heterologous biosynthesis of spinosad: an omics-guided large polyketide synthase gene cluster reconstitution in *Streptomyces*. *ACS Synth Biol* 6:995–1005. <https://doi.org/10.1021/acssynbio.6b00330>.
32. D'Auria JC. 2006. Acyltransferases in plants: a good time to be BAHD. *Curr Opin Plant Biol* 9:331–340. <https://doi.org/10.1016/j.pbi.2006.03.016>.
33. Ruppert M, Woll J, Giritch A, Genady E, Ma X, Stöckigt J. 2005. Functional expression of an ajmaline pathway-specific esterase from *Rauwolfia* in a novel plant-virus expression system. *Planta* 222:888–898. <https://doi.org/10.1007/s00425-005-0031-0>.
34. McGary KL, Slot JC, Rokas A. 2013. Physical linkage of metabolic genes in fungi is an adaptation against the accumulation of toxic intermediate compounds. *Proc Natl Acad Sci U S A* 110:11481–11486. <https://doi.org/10.1073/pnas.1304461110>.
35. Kozakai R, Ono T, Hoshino S, Takahashi H, Katsuyama Y, Sugai Y, Ozaki T, Teramoto K, Teramoto K, Tanaka K, Abe I, Asamizu S, Onaka H. 2020. Acyltransferase that catalyzes the condensation of polyketide and peptide moieties of goadivionin hybrid lipopeptides. *Nat Chem* 12:869–877. <https://doi.org/10.1038/s41557-020-0508-2>.
36. Kieser T, Bibb MJ, Buttner MJ, Chater KF, Hopwood DA. 2000. Practical *Streptomyces* genetics. The John Innes Foundation, Norwich, United Kingdom.
37. Sambrook J, Russell DW. 2001. Molecular cloning: a laboratory manual, 3rd edition. Cold Spring Harbor Laboratory Press, Cold Spring Harbor, NY.
38. Shen J, Kong L, Li Y, Zheng X, Wang Q, Yang W, Deng Z, You D. 2019. A LuxR family transcriptional regulator AniF promotes the production of anisomycin and its derivatives in *Streptomyces hygroscopicus* var. *beijingensis*. *Synth Syst Biotechnol* 1:40–48. <https://doi.org/10.1016/j.synbio.2018.12.004>.
39. Kong L, Zhang W, Chooi YH, Wang L, Cao B, Deng Z, Chu Y, You D. 2016. A multifunctional monooxygenase XanO4 catalyzes xanthone formation in xantholipin biosynthesis via a cryptic demethoxylation. *Cell Chem Biol* 23:508–516. <https://doi.org/10.1016/j.chembiol.2016.03.013>.
40. Zhang W, Wang L, Kong L, Wang T, Chu Y, Deng Z, You D. 2012. Unveiling the post-PKS redox tailoring steps in biosynthesis of the type II polyketide antitumor antibiotic xantholipin. *Chem Biol* 19:422–432. <https://doi.org/10.1016/j.chembiol.2012.01.016>.
41. Thompson JD, Higgins DG, Gibson TJ. 1994. CLUSTAL W: improving the sensitivity of progressive multiple sequence alignment through sequence weighting, position-specific gap penalties and weight matrix choice. *Nucleic Acids Res* 22:4673–4680. <https://doi.org/10.1093/nar/22.22.4673>.
42. Greene TW, Wuts PGM. 1999. Protective groups in organics synthesis. Wiley, New York, NY.
43. Kumar HMS, Reddy BVS, Reddy EJ, Yadav JS. 1999. Iodine-catalyzed mild and efficient tetrahydropyranlation/depyranlation of alcohols. *Chem Lett* 28:857–858. <https://doi.org/10.1246/cl.1999.857>.
44. Kong L, Wang Q, Deng Z, You D. 2020. Characterization of a FAD-dependent halogenase XanH and engineering construction of multifunctional fusion halogenases. *Appl Environ Microbiol* 86:e01225-20. <https://doi.org/10.1128/AEM.01225-20>.
45. Kong L, Wang Q, Yang W, Shen J, Li Y, Zheng X, Wang L, Chu Y, Deng Z, Chooi YH, You D. 2020. Three recently diverging duplicated methyltransferases exhibit substrate-dependent regioselectivity essential for xantholipin biosynthesis. *ACS Chem Biol* 15:2107–2115. <https://doi.org/10.1021/acscchembio.0c00296>.
46. Li Y, Kong L, Shen J, Wang Q, Liu Q, Yang W, Deng Z, You D. 2019. Characterization of the positive SARP family regulator PieR for improving piericidin A1 production in *Streptomyces piomogeeus* var. *Hangzhouwanensis*. *Synth Syst Biotechnol* 4:16–24. <https://doi.org/10.1016/j.synbio.2018.12.002>.
47. Kong L, Liu J, Zheng X, Deng Z, You D. 2019. CtcS, a MarR family regulator, regulates chlortetracycline biosynthesis. *BMC Microbiol* 19:279. <https://doi.org/10.1186/s12866-019-1670-9>.